Direct Measurement of the Return-Current Instability

A. L. Milder,[1,2,3] J. Zielinski,[3] J. Katz,[1] W. Rozmus,[3] D. H. Edgell,[1] A. M. Hansen,[1] M. Sherlock,[4] C. Bruulsema,[3]
J. P. Palastro,[1] D. Turnbull,[1] and D. H. Frolua[1,2]

[1]Laboratory for Laser Energetics, University of Rochester
[2]Department of Physics and Astronomy, University of Rochester
[3]Department of Physics, University of Alberta
[4]Lawrence Livermore National Laboratory

Measurements were made of the return-current instability growth rate, demonstrating its concurrence with nonlocal transport. Thomson scattering was used to measure a maximum growth rate of 5.1×10^9 Hz, which was 3× less than classical Spitzer–Härm theory predicts. The measured plasma conditions indicate the heat flux was nonlocal and Vlasov–Fokker–Planck (VFP) simulations that account for nonlocality reproduce the measured growth rates. Furthermore, the threshold for the return-current instability was measured ($\delta_T = 0.017 \pm 0.002$) to be in good agreement with previous theoretical models.

Significant progress has been made in understanding laboratory and astrophysical plasmas through the use of fluid approximations,[1] but recently an increasing amount of work has been dedicated to understanding the kinetic effects and how the microscale physics impacts the larger macroscopic systems. In particular, kinetic effects associated with nonlocal transport have impacted the interpretation of inertial confinement fusion implosions, laboratory astrophysics, and high-energy-density experiments. Understanding transport and transport-driven instabilities often starts with the classical theories of Spitzer and Härm[2] or Braginskii.[3] Historically, challenges in accounting for kinetic effects, particularly in heat transport, have been addressed with *ad hoc* corrections to the Spitzer–Härm theory in order to match experimental observables.

In a plasma, heat-carrying electrons travel down the temperature gradient (q_{flux}), generating a neutralizing return current (j_{return}) consisting of slower counter-propagating electrons. When the return current is large enough to shift the peak of the electron distribution function beyond the phase velocity of the ion-acoustic waves, the slope of the distribution function becomes inverted and the electrons transfer energy to the waves (inverse Landau damping). These transport-driven waves become absolutely unstable when the inverse Landau damping rate exceeds the ion damping rate.[1] This return-current instability (RCI) is predicted to drive a broad turbulent spectrum of ion-acoustic waves that limit the return current, inhibit heat transport,[4,5] modify laser absorption,[6,7] and alter the fluctuation spectrum from which other ion instabilities grow.[8–10] Previous experimental work has shown anomalous absorption linked to ion turbulence[6] and evidence of reduced heat flux.[5]

In this summary, we present the first measurements of the threshold and linear growth rate of the return-current instability driven by electron heat flux. The thorough characterization of the plasma conditions show that the return-current instability occurs concurrently with nonlocal transport. Thomson scattering was used to measure a maximum RCI growth rate of 5.1×10^9 Hz, which was 3× less than classical Spitzer–Härm theory predicts, but the RCI threshold was measured ($\delta_T = 0.017 \pm 0.002$) to be in good agreement with previous theoretical models.[4,9] Measured plasma conditions indicate that the heat flux was nonlocal and electron velocity distribution functions from VFP simulations, which treat this nonlocality kinetically, reproduce the measured growth rates. These experiments provide a thorough description of the plasma conditions and the associated return-current instability, which enabled detailed comparison with theory and simulations and can now be used to better understand the impact of return-current instability in laboratory and astrophysical plasmas.

A supersonic Mach-3 gas jet with an exit diameter of 2 mm produced an argon gas plume. Eleven 351-nm ultraviolet beams of the OMEGA Laser System were focused 2 mm above the nozzle to heat the plasma. Each beam delivered 200 J in a 1-ns duration full-width at half-maximum (FWHM) flattop pulse. The beams used distributed phase plates, polarization smoothing, and smoothing by spectral dispersion and achieved a peak overlapped intensity of $I_{\text{total}} = 1.1 \times 10^{15}$ W/cm^2.

The overlapped beams produced a hot region of plasma surrounded by a colder region. The overlapped intensity profile created an electron temperature gradient that drove "fast" electrons from the hot region to the cold region. The Thomson-scattered light was collected from various radial locations in the plasma by moving the heater beams and gas jet. The configuration maintained the probed ion-acoustic wave vector parallel to the direction of the heat flux. A distributed phase plate was used on the Thomson-scattering probe beam ($\lambda_0 = 526.5$ nm) to produce a 200-μm FWHM flattop focal spot. This beam was used with ~4 J in a 300-ps FWHM flattop pulse ($I_{2\omega} = 4.2 \times 10^{13}$ W/cm^2) delayed 700 ps from the start of the heater beams to measure spatially resolved Thomson scattering or with ~5 J in a 2-ns FWHM flattop pulse, co-timed with the beginning of the heating beams, and a 100-μm phase plate ($I_{2\omega} = 3.2 \times 10^{13}$ W/cm^2) to measure temporally resolved Thomson scattering. The Thomson-scattering diagnostic, both temporally and spatially resolved, collects light with a 60° scattering angle.

Figure 1 shows the measured temporally resolved ion-acoustic wave amplitudes while the plasma conditions were quasi-stationary (500 to 1000 ps). At 475 μm [Fig. 1(a)], the ion-acoustic wave grows as a function of time consistent with the return-current instability. This is further supported by comparison with growth-rate calculations from the Spitzer–Härm theory and from VFP simulations. The growth rate in the Spitzer–Härm theory was found to be significantly larger than observed in the plasma, which is attributed to the nonlocality of the heat transport. VFP simulations, which include these effects kinetically, show excellent agreement with the data. At a radius of 200 μm [Fig. 1(b)], the ion-acoustic wave decays as a function of time, indicating that the plasma was stable to the return-current instability. The ion-acoustic wave was driven above the thermal fluctuation level at early time, likely by transient RCI or ponderomotive and thermal effects as the plasma was being formed.

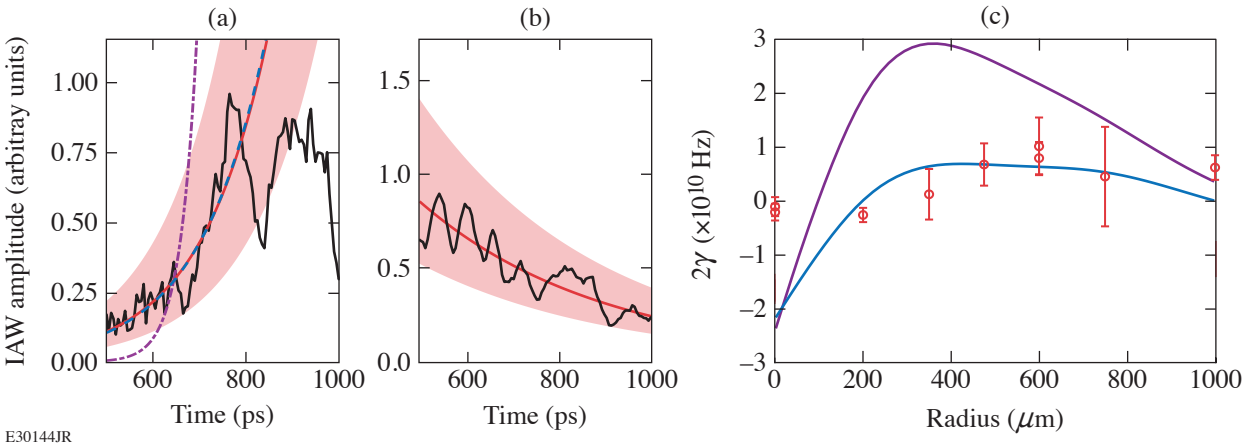

Figure 1
The ion-acoustic wave amplitude (black curves) at a radius of (a) 475 μm and (b) 200 μm are matched with an exponential model (red curves) with a shaded 90% confidence interval. (a) Exponential models with growth rates from the Spitzer–Härm theory (purple curve) and VFP simulations (blue curve) are compared to the data. (c) Measured growth rates (red) are compared to growth rates from the Spitzer–Härm theory (purple curve) and VFP simulations (blue curve) as a function of the radius.

Figure 1(c) compares the ion-acoustic growth rates from simulation and experiment as a function of space. As with the case at 475 μm, the Spitzer–Härm theory overpredicts the growth rate at all spatial locations. Nonlocal transport, included in VFP, was needed to match the measured growth rates. Experiment and simulation showed the return-current instability occurred over a large spatial extent from ~300 to 1000 μm but is maximized around 600 μm where the temperature gradient is large. This association with the temperature gradient helps identify this instability as a transport-driven instability. Simulations predicted the instability

threshold was crossed around 200 μm, while experimental data show the threshold between 200 μm and 350 μm. VFP simulations were performed with the code K2 (Ref. 11) and the resulting distribution functions were used to determine the growth rate.

Calculating the Knudsen number as a function of radius indicates that the return-current instability has a threshold of $\delta_T = 0.017 \pm 0.002$. The Knudsen number is within this range between $r = 200$ μm and $r = 350$ μm where the threshold was noted in Fig. 1(c). The Knudsen number (δ_T) is the scale parameter for the heat-flux distribution function perturbation, and therefore the return-current instability. An analytical threshold for the instability from Tikhonchuk *et al.*[5] is a reliable estimate for the return-current instability threshold. The threshold for the instability is also very close to the threshold for thermal transport nonlocality given by $\delta_T > 0.06/\sqrt{Z}$ (Ref. 12), i.e., RCI will occur where the transport relations are nonlocal.

Heat transport is a ubiquitous process in plasma physics that is impacted by nonlocality and the instabilities it causes. This work has demonstrated the need to account for this nonlocality in the calculation of growth rates for instabilities involving ion-acoustic waves, such as the return-current instability, and to account for the return-current instability under conditions of nonlocal transport. Large spatial extents have been found for both the nonlocal transport and the return-current instability. This can result in changes to instabilities and plasma conditions at a significant distance from the most unstable region. The threshold for the return-current instability was found and is in good agreement with a simple temperature- and density-based model that can be used predictively in future work.

This material is based upon work supported by the Department of Energy National Nuclear Security Administration under Award Number DE-NA0003856, the Office of Fusion Energy Sciences under Award Number DE-SC0016253, the University of Rochester, and the New York State Energy Research and Development Authority. The work of M. Sherlock was performed under the auspices of the U.S. Department of Energy by Lawrence Livermore National Laboratory under Contract DE-AC52-07NA27344.

1. D. W. Forslund, J. Geophys. Res., Space Phys. **75**, 17 (1970).
2. L. Spitzer, Jr. and R. Härm, Phys. Rev. **89**, 977 (1953).
3. S. I. Braginskii, in *Reviews of Plasma Physics*, edited by M. A. Leontovich (Consultants Bureau, New York, 1965), Vol. 1, pp. 205–311.
4. V. T. Tikhonchuk *et al.*, Phys. Plasmas **2**, 4169 (1995).
5. D. R. Gray and J. D. Kilkenny, Plasma Phys. **22**, 81 (1980).
6. S. H. Glenzer *et al.*, Phys. Rev. Lett. **88**, 235002 (2002).
7. W. M. Manheimer, D. G. Colombant, and B. H. Ripin, Phys. Rev. Lett. **38**, 1135 (1977).
8. W. Rozmus *et al.*, Plasma Phys. Control. Fusion **60**, 014004 (2018).
9. A. V. Brantov, V. Yu. Bychenkov, and W. Rozmus, Phys. Plasmas **8**, 3558 (2001).
10. J. D. Moody *et al.*, Phys. Plasmas **7**, 2114 (2000).
11. M. Sherlock, J. P. Brodrick, and C. P. Ridgers, Phys. Plasmas **24**, 082706 (2017).
12. V. Yu. Bychenkov *et al.*, Phys. Rev. Lett. **75**, 4405 (1995).